

Real space renormalization of Majorana fermions in quantum nano-wire superconductors

R. Jafari^{1,2,*}, A. Langari^{3,4}, Alireza Akbari^{1,5,6,†} and Ki-Seok Kim^{5,6}

¹*Asia Pacific Center for Theoretical Physics (APCTP),
Pohang, Gyeongbuk, 790-784, Korea*

²*Department of Physics, Institute for Advanced Studies in Basic Sciences (IASBS), Zanjan 45137-66731, Iran*

³*Department of Physics, Sharif University of Technology, Tehran 14588-89694, Iran*

⁴*Center of Excellence in Complex Systems and Condensed Matter,
Sharif University of Technology, Tehran 14588-89694, Iran*

⁵*Department of Physics, POSTECH,
Pohang, Gyeongbuk 790-784, Korea*

⁶*Max Planck POSTECH Center for Complex Phase Materials,
POSTECH, Pohang 790-784, Korea*

(Dated: November 17, 2015)

We have applied the real space quantum renormalization group approach to study the topological quantum phase transition in the one-dimensional chain of a spinless p-wave superconductor. We investigate the behavior of local compressibility and ground-state fidelity of the Kitaev chain. We show that the topological phase transition is signaled by the maximum of local compressibility at the quantum critical point tuned by the chemical potential. Moreover, a sudden drop of the ground-state fidelity and the divergence of fidelity susceptibility at the topological quantum critical point have been used as a proper indicators for the topological quantum phase transition, which signals the appearance of Majorana fermions. We also present the scaling analysis of ground-state fidelity near the critical point that manifests the universal information about the topological phase transition.

PACS numbers: 71.10.Pm, 64.60.ae, 64.70.Tg, 74.90.+n, 03.67.Lx, 74.45.+c

* rohollah.jafari@gmail.com, jafari@apctp.org

† alireza@apctp.org

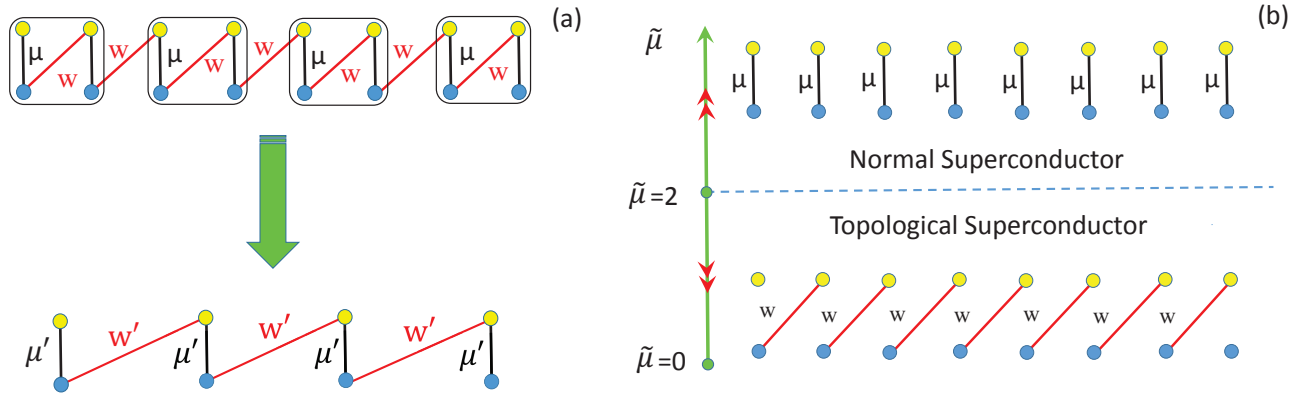


FIG. 1. (Color online.) (a) Renormalization scheme of Majorana fermions in nanowire superconductor, (top) where a block of four MFs is mapped to (bottom) a renormalized pair of MFs. (b) Phase diagram of the one-dimensional Kitaev Model. In this diagram arrows show the flow of chemical potential under RG iteration. Each Majorana mode (yellow circle) for a given site is bound to its partner (blue circle) with strength μ for the normal phase, therefore there are no unbound modes. However for the topological phase there are leaving a free Majorana modes at the ends of a finite size system. In the topological superconductor phase the only existing bonds, with strength w , connect each Majorana mode (yellow circle) to its neighbour partner (blue circle).

I. INTRODUCTION

Majorana fermions (MFs) have attracted intense recent studies in condensed matter systems [1, 2]. MFs are non-abelian anyons, because of exchange statistics [3], which means particle exchanges in general do not commute, and they are nontrivial operations. Furthermore, MFs can be used as qubits in topological quantum computation since they are intrinsically immune to decoherence [4]. There are several promising candidates for practical realization of MFs in one and two dimensional systems. Since a MF is its own antiparticle, it must be an equal superposition of electron and hole states. Hence, superconducting systems are substantial candidates to search for such excitations. MFs can emerge in systems such as topological insulator-superconductor interfaces [5, 6], quantum Hall states with filling factor $5/2$ [7], p-wave superconductors [8], and half-metallic ferromagnets [9, 10].

Among various proposals, the one dimensional (1D) topological nano-wire superconductors (TSCs) [11, 12] provide experimental feasibility for the detection of MFs in hybrid superconductor-semiconductor wires [13, 14]. An egregious feature of a 1D TSC is the edge states (MFs), which appear at the ends of the superconducting wire. As shown by Kitaev [15], MFs can appear at the ends of 1D spinless p-wave superconducting chain when the chemical potential is less than a finite value, i.e. being in the topological regime. Recent progress in spin-orbit coupling research makes it possible to realize Kitaev chain in hybrid systems, such as superconductor-topological insulator interface [5], or semiconductor-superconductor heterostructure [2, 16, 17]. In such hybrids, a one dimensional spin-orbit coupling nanowire is proximity coupled to an ordinary s-wave superconductor [11, 12]. It was predicted that there is a topological quantum phase transition (TQPT) in the system whenever a proper Zeeman field is applied, where the zero-energy modes and MFs appear in the topological non-trivial phase. All these experimental observations of the existence of Majorana fermions rely on the fact that the system is in the topological phase. Moreover, the observation of Majorana fermions has been reported using scanning tunneling microscopy [18]. In addition, a topological phase can not be described within the Landau-Ginzburg symmetry breaking paradigm, which makes the investigation of such systems being complicated. This fact has led to various types of approximations schemes, which can be roughly classified as variational, perturbative, numerical and renormalization group techniques. The difficulty of the task suggests perhaps that one should combine various techniques in order to come as close as possible to the exact solution.

In this paper, we have applied the real space quantum renormalization group (QRG) approach to acquire the topological phase transition of the one dimensional p-wave superconductor. We also calculate the local compressibility, ground-state fidelity, and fidelity susceptibility of the model as the robust geometric probes of quantum criticality. Ground-state fidelity is a measure, which shows the qualitative change of the ground state properties without the need to know a prior knowledge of the underlying phases. The universal scaling properties of fidelity and fidelity susceptibility have been investigated to extract the universal information of the topological phase transition.

The paper is organized as follows: In the next section, the model and majorana fermions are introduced. In Section III, the quantum renormalization approach is introduced to study the ground state phase diagram of the model. In section. IV, the density of particle and compressibility are investigated and section V is dedicated to analysis the ground state fidelity, fidelity susceptibility, and universal behaviour of the fidelity. Finally, we will discuss and summarize our results in Section VI.

II. ONE DIMENSION QUANTUM NANO-WIRE SUPERCONDUCTORS

The Kitaev model, which was the first model realizing MFs in a one dimensional lattice [15], is given by following Hamiltonian

$$\mathcal{H} = \sum_{m=1} \left[-\mu c_m^\dagger c_m - w(c_m^\dagger c_{m+1} + c_{m+1}^\dagger c_m) + \Delta(c_m c_{m+1} + c_{m+1}^\dagger c_m^\dagger) \right], \quad (1)$$

where μ is the chemical potential, c_m^\dagger and c_m are the electron creation and annihilation operators on site m . The superconducting gap, and hopping integral are defined by Δ and w respectively. Since the time-reversal symmetry is broken in Eq. (1), we only consider a single value spin projection, i.e., effectively spinless electrons.

By introducing Majorana fermion operators as $a_n = c_n + c_n^\dagger$ and $b_n = i(c_n^\dagger - c_n)$, which satisfy the communication relations: $\{a_m, a_n\} = \{b_m, b_n\} = 2\delta_{m,n}$ and $\{a_m, b_n\} = 0$, the Hamiltonian, Eq. (1), takes the following form

$$\mathcal{H} = \frac{-iw}{2} \sum_{n=1} \left[\tilde{\mu} a_n b_n + (1 - \tilde{\Delta}) a_n b_{n+1} + (1 + \tilde{\Delta}) a_{n+1} b_n \right], \quad (2)$$

where $\tilde{\Delta} = \Delta/w$, and $\tilde{\mu} = \mu/w$. It is well-known [15] that for the case $|\mu| < 2w$, the ground state with MFs is fully realised and the system is called a topological superconductor, which shows qualitatively different behavior from the trivial phase, $|\mu| > 2w$, without Majorana fermions.

III. QUANTUM RENORMALIZATION GROUP

Quantum renormalization group is a method of studying systems with a large number of strongly correlated degrees of freedom. The main idea of this method is to decrease or thinning the number of degrees of freedom, so as to retain the information about essential physical properties of the system and eliminate those features which are not important for the considered phenomena. In the real space QRG, which is usually performed on lattice systems with discrete variables, one can divide the lattice into blocks which are treated as the sites of the new lattice. The Hamiltonian is divided into intra-block and inter-block parts, the former being exactly diagonalized, and a number of low lying energy eigenstates are kept to project the full Hamiltonian onto the new lattice [19–25]. In the new system there are less degrees of freedom, and the renormalized couplings are expressed as functions of the initial system's couplings. Analysing the renormalized couplings (by tracing the flow of coupling constants), one can determine qualitatively the structure of the phase diagram of the underlying system, and approximately locate the critical points (unstable fixed points), and different phases (corresponding to stable fixed points). We emphasise that this is a technically simple method which produces qualitative correct results when properly applied. Moreover, it is convenient to carry out analytical calculation in the lattice models and they are technically easy to extend to the higher dimensions.

To implement the idea of QRG, the Hamiltonian, Eq. (2), is divided into blocks of four MFs sites, as shown in Fig. 1(a). In this case, the total intra-blocks Hamiltonian is given by $\mathcal{H}_B = \sum_{I=1}^{N/2} h_I^B$, with

$$h_I^B = \frac{-iw}{2} \left[\tilde{\mu} a_{1,I} b_{1,I} + \tilde{\gamma} a_{1,I} b_{2,I} + \tilde{\lambda} a_{2,I} b_{1,I} \right], \quad (3)$$

where $\tilde{\gamma} = 1 - \tilde{\Delta}$, $\tilde{\lambda} = 1 + \tilde{\Delta}$, and the remaining part of the Hamiltonian is included in the inter-block part

$$\mathcal{H}_{BB} = \frac{-iw}{2} \sum_{I=1}^{N/2} \left[\tilde{\mu} a_{2,I} b_{2,I} + \tilde{\gamma} a_{2,I} b_{1,I+1} + \tilde{\lambda} a_{1,I+1} b_{2,I} \right],$$

where we consider the open boundary chain.

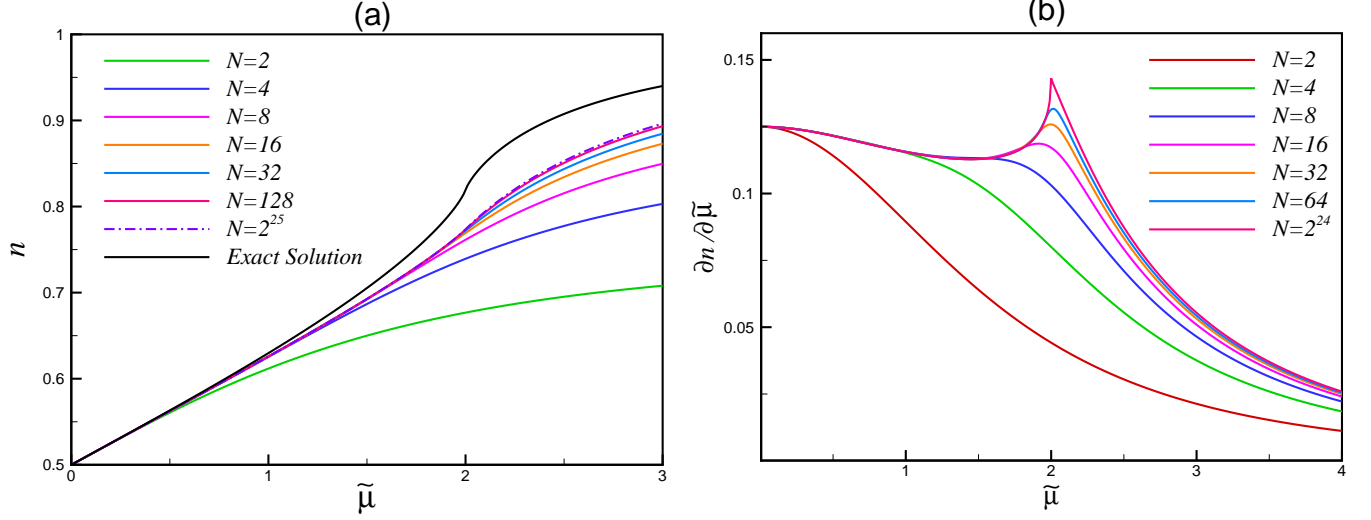


FIG. 2. (Color online.) (a) The particle density n versus chemical potential μ for different system sizes (the exact solution data has been taken from Ref. 26). (b) Derivative of particle density with respect to chemical potential (compressibility) versus μ for different lattice sizes.

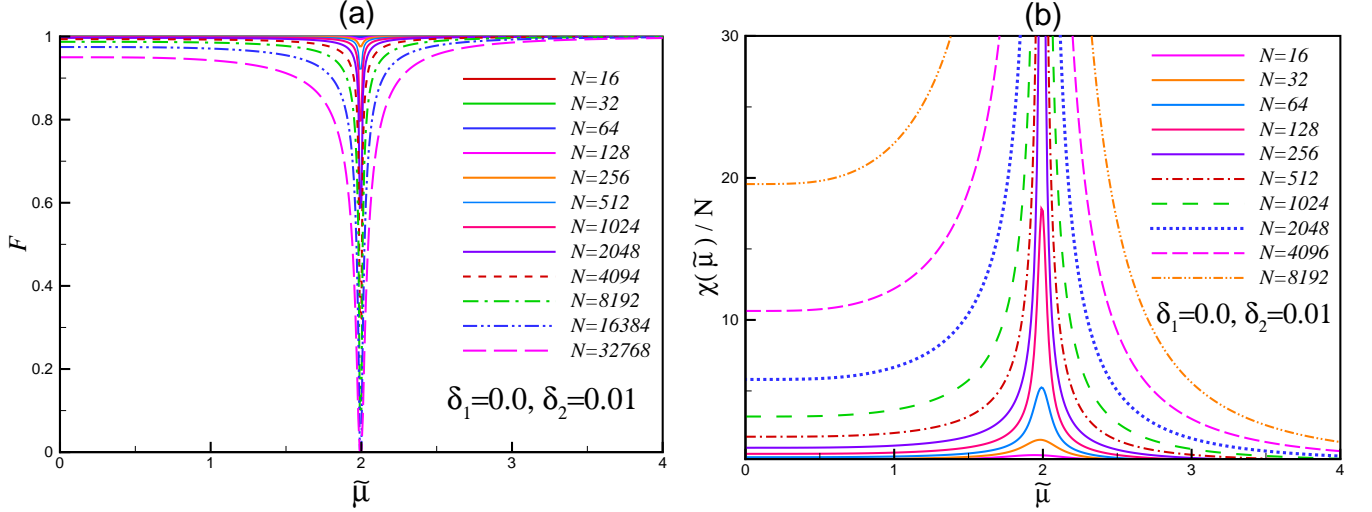


FIG. 3. (Color online.) (a) Evaluation of the ground state fidelity of superconducting nanowire under quantum renormalization group for different chain sizes. (b) Fidelity of susceptibility per lattice size for different chain sizes.

The eigenstates and eigenvalues of the block Hamiltonian of four MFs are given by

$$\begin{aligned}
 |\psi_0\rangle &= \frac{\alpha_0}{2}(a_1 - ib_1)|0_1^{a,b}, 0_2^{a,b}\rangle + \frac{\beta_0}{2}(a_2 - ib_2)|0_1^{a,b}, 0_2^{a,b}\rangle, \quad |\psi_1\rangle = \beta_1|0_1, 0_2\rangle - \frac{\alpha_1}{4}(a_1 - ib_1)(a_2 - ib_2)|0_1^{a,b}, 0_2^{a,b}\rangle, \\
 |\psi_2\rangle &= \alpha_1|0_1, 0_2\rangle + \frac{\beta_1}{4}(a_1 - ib_1)(a_2 - ib_2)|0_1^{a,b}, 0_2^{a,b}\rangle, \quad |\psi_3\rangle = \frac{\beta_0}{2}(a_1 - ib_1)|0_1^{a,b}, 0_2^{a,b}\rangle - \frac{\alpha_0}{2}(a_2 - ib_2)|0_1^{a,b}, 0_2^{a,b}\rangle,
 \end{aligned} \quad (4)$$

and

$$E_0 = -\frac{w}{2}(\tilde{\mu} + \sqrt{\tilde{\mu}^2 + 4}), \quad E_1 = -\frac{w}{2}(\tilde{\mu} + \sqrt{\tilde{\mu}^2 + 4\tilde{\Delta}^2}), \quad E_2 = -\frac{w}{2}(\tilde{\mu} + \sqrt{\tilde{\mu}^2 - 4\tilde{\Delta}^2}), \quad E_3 = -\frac{w}{2}(\tilde{\mu} - \sqrt{\tilde{\mu}^2 + 4}), \quad (5)$$

respectively. Here $|0_1^{a,b}, 0_2^{a,b}\rangle$ is the vacuum state of MFs in real space and

$$\alpha_0 = -\frac{E_0/w}{\sqrt{(E_0/w)^2 + 1}}, \quad \beta_0 = \frac{1}{\sqrt{(E_0/w)^2 + 1}}, \quad \alpha_1 = -\frac{E_1/w}{\sqrt{(E_1/w)^2 + \tilde{\Delta}^2}}, \quad \beta_1 = \frac{\tilde{\Delta}}{\sqrt{(E_1/w)^2 + \tilde{\Delta}^2}}.$$

The projection operator P_0^I for the I -th block is defined by $P_0^I = |\psi_0\rangle_{II}\langle\psi_0| + |\psi_1\rangle_{II}\langle\psi_1|$, and the renormalization of MFs operators are given by

$$\begin{aligned} P_0^I a_{1,I} P_0^I &= (\alpha_1 \beta_0 + \alpha_0 \beta_1) a_I, & P_0^I a_{2,I} P_0^I &= (\beta_0 \beta_1 - \alpha_1 \alpha_0) a_I, \\ P_0^I b_{1,I} P_0^I &= (\alpha_1 \beta_0 - \alpha_0 \beta_1) b_I, & P_0^I b_{2,I} P_0^I &= (-\alpha_1 \alpha_0 - \beta_0 \beta_1) b_I. \end{aligned} \quad (6)$$

In this respect the effective Hamiltonian is expressed by

$$\mathcal{H}^{eff} = P_0(\mathcal{H}_B + \mathcal{H}_{BB})P_0, \quad (7)$$

with total projector $P_0 = \bigotimes_{I=1}^N P_0^I$. Thus, the effective Hamiltonian is obtained

$$\mathcal{H}^{eff} = -\frac{i}{2} \sum_{n=1} w' \left[\tilde{\mu}' a_n b_n + (-1 + \tilde{\Delta}') a_n b_{n+1} - (1 + \tilde{\Delta}') a_{n+1} b_n \right] + e_0, \quad (8)$$

where w' , $\tilde{\mu}'$, and $\tilde{\Delta}'$ are the renormalized coupling constants defined by

$$w' = w[\alpha_0 \beta_0 + \tilde{\Delta} \alpha_1 \beta_1], \quad \tilde{\Delta}' = -\frac{w}{w'}[\alpha_1 \beta_1 + \tilde{\Delta} \alpha_0 \beta_0], \quad \tilde{\mu}' = \frac{(E_1 - E_0) - \mu(\alpha_1^2 - \beta_0^2)}{w'}, \quad (9)$$

and $e_0 = E_0 - \mu\beta_0^2$ is a constant term as a function of coupling constants.

Apart from the constant term, the effective Hamiltonian of the renormalized chain is not exactly similar to the original one since the sign of hopping term and superconducting gap have been changed. To get a self-similar Hamiltonian, we implement the unitary transformation $a_n \rightarrow (-1)^n a_n$, and $b_n \rightarrow (-1)^n b_n$, which is equivalent to π rotation of even (or odd) sites around z -axis. We should emphasise that the commutation relations of MFs operators do not change under these transformation.

The stable and unstable fixed points of the QRG equations are obtained by solving the following equations $\tilde{\mu}' = \tilde{\mu}$, and $\tilde{\Delta}' = \tilde{\Delta}$. For simplicity we take $\Delta = w$, for which the Jordan Wigner transformation transforms this model to the Ising model in a transverse field.

For $\tilde{\Delta} = 1$ the renormalized couplings reduce to $w' = 2w/\sqrt{4 + \tilde{\mu}^2}$, and $\tilde{\mu}' = \tilde{\mu}^2/2$. The QRG equations show that the stable fixed points are located at $\tilde{\mu} = 0$ and $\tilde{\mu} \rightarrow \infty$ while $\tilde{\mu}_c = 2$ stands for the unstable fixed point, which specifies the quantum critical point of the model. The phase diagram of the model has been shown in Fig. 1(b). As depicted, the chemical potential goes to zero for $\tilde{\mu} < \tilde{\mu}_c$ under QRG transformation, while it scales to infinity in the normal superconductor phase. The QRG equations, Eq. (9), show the flow of w to zero in a normal superconductor, which represents the renormalization of the energy scale while it goes to 1 for the topological superconductor. Fig. 1(b) shows that in the topological superconductor phase the only existing bonds connect a_n to its neighbor b_{n+1} , and the Majorana modes at the ends of the chain are not coupled to anything. It manifests the presence of edge modes of a topological phase, which is the reason for the ground-state degeneracy that is not due to a symmetry. Furthermore, we see in the normal superconductor phase, each Majorana mode a_n on a given site is bound to its partner b_n with strength μ , leaving no unbound modes, i.e. no edge state.

The quantum critical exponents associated with this quantum critical point can be obtained from the Jacobian of the QRG transformations by linearizing the QRG flow at the critical point ($\tilde{\Delta} = 1$, and $\tilde{\mu} = 2$),

$$J = \begin{pmatrix} \frac{\partial \tilde{\mu}'}{\partial \mu} & \frac{\partial \tilde{\mu}'}{\partial \tilde{\Delta}} \\ \frac{\partial \tilde{\Delta}'}{\partial \mu} & \frac{\partial \tilde{\Delta}'}{\partial \tilde{\Delta}} \end{pmatrix}, \quad (10)$$

which yields

$$J = \begin{pmatrix} 2 & -1 \\ 0 & 0 \end{pmatrix}. \quad (11)$$

The eigenvalues of the matrix of linearized flow are $\eta_1 = 2$ and $\eta_2 = 0$. The corresponding eigenvectors in the $|\tilde{\mu}, \tilde{\Delta}\rangle$ coordinates are $|\eta_1\rangle = |1, 0\rangle$, $|\eta_2\rangle = |1, 2\rangle$. $|\eta_1\rangle$ shows the relevant direction which represents the direction of flow of chemical potential (see Fig. 1(b)). We have also calculated the correlation length exponents at the critical point $\tilde{\mu}_c = 2$. In this respect, the correlation length diverges as $\xi \sim |\tilde{\mu} - 2|^{-\nu}$ with the exponent $\nu = 1$, which is expressed by $\nu = \ln[n_B]/\ln[d\tilde{\mu}'/d\tilde{\mu}]|_{\tilde{\mu}_c}$, where $n_B = 2$ is the number of sites in each block.

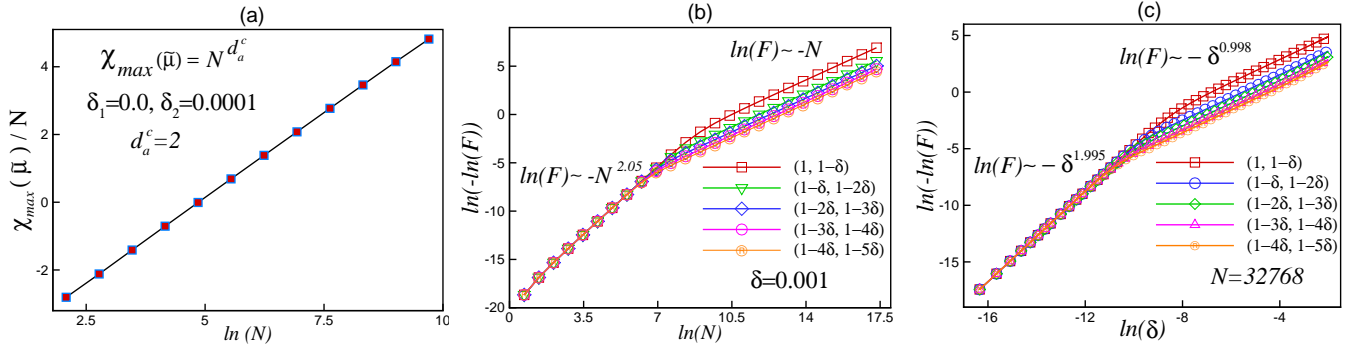


FIG. 4. (Color online.) (a) The scaling behavior of the maximum of fidelity susceptibility in terms of system size. (b) Scaling behavior of the ground state fidelity, $\ln(-\ln(F))$, versus $\ln(N)$ close to the critical point $\tilde{\mu}_c = 2$, for the Kitaev model with fixed $\delta = 0.001$. (c) Scaling behavior of $\ln(-\ln(F))$ versus $\ln(\delta)$ for fixed size $N = 2^{15}$ close to $\tilde{\mu}_c = 2$.

IV. PARTICLE DENSITY

The average local density of particles on site n is $n(\tilde{\mu}) = \frac{1}{N} \sum_{n=1} \langle \Psi_0 | \frac{(a_n - ib_n)(a_n + ib_n)}{4} | \Psi_0 \rangle$. The ground state of the renormalized chain is related to the ground state of the original one by the transformation $P_0 |\Psi'_0\rangle = |\Psi_0\rangle$. This leads to the particle density in the renormalized chain

$$n(\tilde{\mu}, N) = \frac{1}{N} \sum_{n=1} \langle O' | P_0 \left(\frac{(a_n - ib_n)(a_n + ib_n)}{4} \right) P_0 | O' \rangle = \frac{1}{2} + \gamma(0) n(\tilde{\mu}', \frac{N}{2}), \quad (12)$$

where $n(\tilde{\mu}', N/2)$ is the particle density in the renormalized chain and $\gamma(0)$ is defined by $(2\alpha_1^2 - 1)/2$.

The average of the local density of particles has been plotted in Fig. 2(a) for different system sizes. It has been compared with the known exact result [26], which shows good agreement qualitatively. The compressibility, derivative of the local density of particles with respect to chemical potential, has been depicted in Fig. 2(b). The non-analytic behavior of the particle density at $\tilde{\mu}_c = 2$ is high-lighted in the divergent behavior of the corresponding compressibility, which shows the existence of the quantum critical point. It clearly represents that the compressibility has a singularity at the topological critical point in the thermodynamic limit ($N \rightarrow \infty$).

V. GROUND STATE FIDELITY

In the last few years, fidelity, which is a measure of the distance between quantum states, has been accepted as a new notion to characterize the drastic change of the ground states in quantum phase transition (QPT) point. Unlike traditional approaches, prior knowledge about the symmetries and order parameters of the model are not required in the fidelity notion to find out a QPT. In addition, fidelity has an interdisciplinary role, for example, it is related to the density of topological defects after a quench [27, 28], decoherence rate of a test qubit interacting with a non-equilibrium environment [29, 30], and orthogonality catastrophe of condensed matter systems [31]. In this section, we implement the formalism introduced in Refs. [32 and 33] to calculate the ground state fidelity of the nano-wire superconductor in terms of quantum renormalization group. The advantage of the formalism is its capability to evaluate the fidelity of a model without referring to the exact ground state of the model.

The fidelity of ground state is defined by the overlap between the two ground state wave functions at different parameter values as follows

$$F = \langle \Psi_0(\tilde{\mu} - \delta_1) | \Psi_0(\tilde{\mu} + \delta_2) \rangle = \langle \Psi_0(\tilde{\mu}_-) | \Psi_0(\tilde{\mu}_+) \rangle, \quad (13)$$

where δ_j ($j = 1, 2$) is a small deviation in the chemical potential. According to the renormalization transformation $P_0 |\Psi'_0\rangle = |\Psi_0\rangle$, the fidelity of renormalized chain are related to the fidelity of original Hamiltonian by $F(\tilde{\mu}, N) = \gamma_1 F(\tilde{\mu}', N/2)$, where $\gamma_1 = \left(\alpha_0(\tilde{\mu}_-) \alpha_0(\tilde{\mu}_+) + \beta_0(\tilde{\mu}_-) \beta_0(\tilde{\mu}_+) \right)^{\frac{N}{2}}$. The ground state fidelity of the model has been plotted versus chemical potential in Fig. 3(a) for different system sizes. Obviously, the ground state fidelity shows a sudden drop at the topological quantum critical point. Increasing the system size increases the depth of drop, which manifests unflinching drop in the thermodynamic limit. To determine more precisely the effect of quantum criticality on fidelity,

we should extract universal information about the transition in addition to providing the location of the critical point. The universal information is defined by the critical exponents and reflects symmetries of the model rather than its microscopic details. For small system size, the universal information is explored in the fidelity susceptibility (χ) approach,[28, 34, 35] which is defined by

$$\chi = 2 \lim_{\delta \rightarrow 0} \frac{1 - F}{\delta^2}, \quad (14)$$

in which $\delta_1 = \delta_2 = \delta/2$ is supposed. Fig. 3(a) represents fidelity susceptibility (FS) per lattice size (χ/N) versus chemical potential, for various system sizes. Although χ/N does not show divergence for finite lattice sizes, the curves display marked anomalies with the height of peaks increasing with system size and diverges in the thermodynamics limit as the critical point is touched. The maximum of FS at finite size lattice N obeys the scaling $\chi_{max} = N^{d_a^c}$ where d_a^c denotes the critical adiabatic dimension[36, 37]. The scaling analysis of FS is figured out in Fig. 4(a). It is clearly verified that the scaling relation $\chi_{max} = N^{d_a^c}$ is satisfied with $d_a^c = 2$. It is worth to mention that, the critical adiabatic dimension for the Ising model in a transverse field (ITF) is $d_a^c = 2$ [36, 37]. Furthermore, it has been shown that in the thermodynamic limit at fixed δ , the fidelity scaling is given by[35]

$$\ln F(\tilde{\mu}, \delta) \sim -N|\delta|^{d\nu} g\left(\frac{\tilde{\mu} - \tilde{\mu}_c}{\delta}\right), \quad (15)$$

where g is a scaling function. It has been shown that[35] at the critical point, fidelity is non-analytic in δ as $\ln F(\tilde{\mu}_c, \delta) \sim -N|\delta|^{d\nu}$, while away from critical point for $|\delta| \ll |\tilde{\mu} - \tilde{\mu}_c| \ll 1$, it behaves as

$$\ln F(\tilde{\mu}_c, \delta) \sim -N\delta^2 |\tilde{\mu} - \tilde{\mu}_c|^{d\nu-2}. \quad (16)$$

The scaling behavior of fidelity around the critical point, $\tilde{\mu} \approx \tilde{\mu}_c$, is depicted in Fig. 4 (b). As seen, for small system sizes we have obtained the well known result [35] $\ln F \sim -N^2$, reported for ITF model in the finite size scaling case [34]. However for larger system sizes, we obtain $\ln F \sim -N$ conforming to Eq. (15). A more detailed analysis shows that the transition between the two regimes takes place when $N|\delta| \sim 1$. For this purpose we have plotted in the Fig. 4(c), the scaling behavior of $\ln(-\ln F)$ versus $\ln(\delta)$ when the system size is kept fixed. We observe two distinct regimes, namely for $N|\delta| \ll 1$ we have $\ln F \sim -\delta^2$, and for $N|\delta| \gg 1$ we find $\ln F \sim -|\delta|$ in agreement with Eqs. (15) and (16). It should be mentioned that in our model $d = 1$ and scaling verifies the correlation length exponent of $\nu = 1$, which exactly corresponds to the correlation length exponent of ITF model.

VI. SUMMARY AND CONCLUSIONS

In this work we have presented real space quantum renormalization of Majorana fermions to obtain the phase diagram, compressibility, ground state fidelity and scaling behavior of fidelity susceptibility. For the special case, where the hopping term equals the pairing term the Kitaev model is mapped to the Ising model in a transverse field. We have analyzed the scaling behavior of the Kitaev model in the mentioned case. We show that real space quantum renormalization group procedure could reproduce exactly the location of the critical point and the critical exponents. The result shows that in the topological phase ($\tilde{\mu} < \tilde{\mu}_c = 2$) the chemical potential goes to zero by renormalization iteration while in the normal superconductor phase it flows to infinity. Furthermore, our results show that the correlation length exponent and the critical adiabatic dimension are $\nu = 1$ and $d_a^c = 2$, respectively, corresponding to their counterpart in the Ising model in transverse field.

ACKNOWLEDGMENTS

We are grateful to S. Kettemann, V. Dobrosavljevic, B. Kamble for fruitful discussions and feedbacks. A.A. acknowledges support by Max Planck POSTECH / KOREA Research Initiative (No. 2011-0031558) programs through NRF funded by MSIP of Korea.

-
- [1] C. Nayak, S. H. Simon, A. Stern, M. Freedman, and S. Das Sarma, Rev. Mod. Phys. **80**, 1083 (2008).
 - [2] A. Jason, Reports on Progress in Physics **75**, 076501 (2012).
 - [3] S. Ady, Nature **464**, 187 (2010).

- [4] A. Y. Kitaev, *Annals of Physics* **303**, 2 (2003).
- [5] L. Fu and C. L. Kane, *Phys. Rev. Lett.* **100**, 096407 (2008).
- [6] J. Linder, Y. Tanaka, T. Yokoyama, A. Sudbø, and N. Nagaosa, *Phys. Rev. Lett.* **104**, 067001 (2010).
- [7] M. Gregory and R. Nicholas, *Nuclear Physics B* **360**, 362 (1991).
- [8] N. Read and D. Green, *Phys. Rev. B* **61**, 10267 (2000).
- [9] M. Duckheim and P. W. Brouwer, *Phys. Rev. B* **83**, 054513 (2011).
- [10] S. B. Chung, H.-J. Zhang, X.-L. Qi, and S.-C. Zhang, *Phys. Rev. B* **84**, 060510 (2011).
- [11] R. M. Lutchyn, J. D. Sau, and S. Das Sarma, *Phys. Rev. Lett.* **105**, 077001 (2010).
- [12] Y. Oreg, G. Refael, and F. von Oppen, *Phys. Rev. Lett.* **105**, 177002 (2010).
- [13] V. Mourik, K. Zuo, S. M. Frolov, S. R. Plissard, E. P. A. M. Bakkers, and L. P. Kouwenhoven, *Science* **336**, 1003 (2012).
- [14] M. T. Deng, C. L. Yu, G. Y. Huang, M. Larsson, P. Caroff, and H. Q. Xu, *Nano Letters* **12**, 6414 (2012), pMID: 23181691.
- [15] A. Kitaev, *Physics-Uspekhi* **44**, 131 (2001).
- [16] J. D. Sau, R. M. Lutchyn, S. Tewari, and S. Das Sarma, *Phys. Rev. Lett.* **104**, 040502 (2010).
- [17] C. W. J. Beenakker, *Annu Rev Cond Phys* **4**, 113 (2013).
- [18] S. Nadj-Perge, I. K. Drozdov, J. Li, H. Chen, S. Jeon, J. Seo, A. H. MacDonald, B. A. Bernevig, and A. Yazdani, *Science* **346**, 602 (2014).
- [19] A. Langari, *Phys. Rev. B* **69**, 100402 (2004).
- [20] R. Jafari and A. Langari, *Physica A* **364**, 213 (2006).
- [21] R. Jafari and A. Langari, *Phys. Rev. B* **76**, 014412 (2007).
- [22] R. Jafari, M. Kargarian, A. Langari, and M. Siahatgar, *Phys. Rev. B* **78**, 214414 (2008).
- [23] R. Jafari, *Phys. Rev. A* **82**, 052317 (2010).
- [24] R. Jafari, *Physics Letters A* **377**, 3279 (2013).
- [25] A. Langari and V. Karimipour, *Physics Letters A* **236**, 106 (1997).
- [26] D. Nozadze and N. Trivedi, *arXiv:1504.00013* (2015).
- [27] B. Damski, *Phys. Rev. Lett.* **95**, 035701 (2005).
- [28] R. Jafari, *arXiv:1503.08719* (2015).
- [29] B. Damski, H. T. Quan, and W. H. Zurek, *Phys. Rev. A* **83**, 062104 (2011).
- [30] R. Jafari and A. Akbari, *EPL (Europhysics Letters)* **111**, 10007 (2015).
- [31] P. W. Anderson, *Phys. Rev. Lett.* **18**, 1049 (1967).
- [32] A. Langari and A. T. Rezakhani, *New Journal of Physics* **14**, 053014 (2012).
- [33] N. Amiri and A. Langari, *physica status solidi (b)* **250**, 537 (2013).
- [34] P. Zanardi and N. Paunković, *Phys. Rev. E* **74**, 031123 (2006).
- [35] M. M. Rams and B. Damski, *Phys. Rev. Lett.* **106**, 055701 (2011).
- [36] S.-J. GU, *Int. J. Mod. Phys. B* **24**, 4371 (2010).
- [37] W.-C. Yu, H.-M. Kwok, J. Cao, and S.-J. Gu, *Phys. Rev. E* **80**, 021108 (2009).